Songklanakarin J. Sci. Technol.
40 (4), 921-927, Jul. - Aug. 2018

http://www.sjst.psu.ac.th

Original Article

Biosorption of Rhodamine B by organo-pomelo peel: Kinetic, mechanistic and thermodynamic studies

Chakkrit Umpuch* and Sripattra Sopasin

Department of Chemical Engineering, Faculty of Engineering,
Ubon Ratchathani University, Warin Chamrap, Ubon Ratchathani, 34190 Thailand

Received: 20 November 2016; Revised: 11 May 2017; Accepted: 22 May 2017

Abstract

This work investigated the potential use of organo-pomelo peel(OPP) biomass prepared by adsolubilization to remove Rhodamine B (RB), a common dye in industries, from aqueous solutions. The OPP and precursor were characterized by Brunauer-Emmett-Teller method, Fourier transform infrared spectrometer, and scanning electron microscope. The biosorption of RB strongly depends on the initial dye concentration, pH, temperature, and contact time. The optimum condition was observed at pH6.0, 35°C and 40 min. The equilibrium data was analyzed by using Langmuir, Freundlich, and Temkin isotherm models. The pseudo-first order, pseudo-second order, and intra particle kinetic models were applied to study the kinetic behavior. The thermodynamic study showed that the biosorption process was exothermic and spontaneous. Results indicated that the OPP was an effective adsorbent for removal of RB from aqueous solution.

Keywords: adsolubilization, organo-pomelo peel, Rhodamine B, biosorption, organophilicity

1. Introduction

Many industries, such as paper and pulp, cosmetics, paint and pigments, plastics, leather tanning, and textile industries, release large amounts of wastewater contaminated by various synthetic dyes and heavy metals. This wastewater causes toxic and aesthetic problems, and poor sunlight penetration into the water reduces photosynthetic activity of aquatic plants (Rao *et al.*, 2010). The synthetic dye Rhodamine B (RB) is one of the most common dyes used in above industries, and it is harmful to humans and animals, causing irritation to the skin, eyes, and respiratory tract (Pehlivan & Altun, 2007). Experiments have shown it to be carcinogenicity and toxic to reproductive, developmental, and neurological systems in humans and animals (Umpuch, 2015). Thus, the removal of RB from industrial effluent is an important step in environmental welfare.

*Corresponding author
Email address: chakkrit.u@ubu.ac.th

Many developing techniques have been taken for removing RB from wastewater, including filtration, advanced oxidation, electrolysis and microbial degradation (Tasaso, 2014; Umpuch & Sakaew, 2013). Although these methods were efficient, there were a number of limitations for the treatment of effluent containing RB molecules because these molecules are structurally complex and resistant to heat and light. The adsorption process, a simple method with high adsorbing capacity for soluble contaminants in water, provides an attractive and alternative treatment, especially if the adsorbent is cheap and readily available. Activated carbon is a well-known adsorbent for the removal of synthetic dyes from wastewater but it involves high energy consumption in the preparation stage and has low reutilization (Khan *et al.*, 2013). Consequently, many investigators studied the feasibility of using low cost and alternative materials like coconut shell, natural clay, chitin, bagasse pith, banana pith, tea leaves, saw dust, orange peel, and lemon peel as biosorbents for removal of RB from wastewater (Pagnanelli *et al.*, 2013; Umpuch & Jutarat, 2013).

Citrus grandis (Pomelo) is common in many parts of Thailand. It is a large citrus fruit, about 15 to 25 cm in diameter, usually pale green to yellow (flavedo) when ripe,

with sweet white flesh and very thick albedo (rind pith). Pomelo peel (PP) is abundant throughout the year around the country and finishes up as solid waste. The development of biosorbent from PP reduces the cost of solid waste management and provides an alternative sorbent to the existing commercial activated carbon. PP is composed of soluble and insoluble monomers and polymers (Tasaso, 2014). These polymers contain carboxylic and hydroxyl groups which can interact cationic species including dyes and heavy metals (Anastopoulos & Kyzas, 2014).

Recently reports stated that it was possible that the adsorption capacity of dyes onto biosorbents was greatly improved by adsolubilisation (Hameed, 2009), a process in which the long chain cationic surfactant was loaded on the external surface and interior surfaces of the precursor by electrostatic attraction, which results in the adsorbent surface altering from hydrophilic to organophilic and is known as "organo-adsorbent" (Schiewer & Iqbal, 2010). There have been many attempts to develop surfactant-modified adsorbent from agricultural residues, such as rice straw, bagasse, and corn straw. These surfactant-modified biosorbents showed increased anionic dyes uptake (Bhat *et al.*, 2015; Ma *et al.*, 2016). However, literature on the adsorption of cationic dye such as RB using surfactant-modified biomass-based adsorbents and its binding interactions has not been well documented.

As a result, this study focused on a development of novel and low-cost biosorbent, such as organo-pomelo peel (OPP), to remove RB from wastewater. Factor influencing adsorption ability such as initial concentration, pH, temperature, and contact time were monitored to identify optimal conditions.

2. Material and Methods

2.1 Preparation of synthetic sample

A parent solution of RB (1,000 mg/L) was prepared by dissolving appropriate quantity of RB (C.I. 45170, LOBA Chemie, India) in distilled water. The molecular weight of RB is 479.01 g/mol. The stock dye solution was diluted to obtain the required initial concentrations (50-300 mg/L). The chemical structure of RB is illustrated in Figure 1. Hexadecyltrimethyl ammonium bromide (HDTMA; Fluka, Sigma-Aldrich, India), was used as cationic surfactant. HDTMA solution (2.0 g/L) was prepared by dissolving in distillated water.

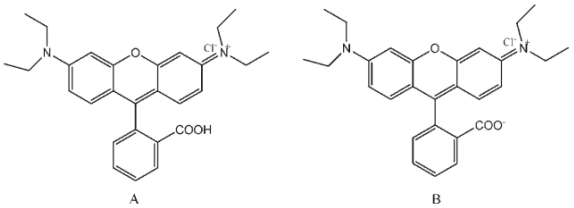

Figure 1. Structures of Rhodamine B in tis (A) cationic, and (B) zwitterionic forms (Ma *et al.*, 2016).

2.2 Collection and preparation of adsorbent

The PP residual biomass was obtained from a local market near Ubon Ratchathani University, Thailand. Initially PP was air dried in sunlight for 24 hrs and then washed thoroughly with tap water to remove dust and other impurities. The dried precursor was crushed and sieved to obtain particle size below 300 micron. Finally, the adsorbent was dried at 60°C until its weight was constant and stored in a desiccator for further use. An amount of 1.0 g of the precursor was added to 100 mL of 2 g/L HDTMA solution which was contained in a 250 mL Erlenmeyer flask. The flasks were horizontally shaken at 200 rpm for 24 hrs at room temperature. The OPP was harvested from the suspension by filtering through a vacuum micro-filter and washed several times with distilled water until the pH solution and conductivity were constant. The OPP was dried in an oven at 60 °C for 24 hrs and stored in a desiccator for further use.

2.3 Adsorption experiments

From our preliminary study, the percentages of RB removal of the PP and OPP were 4.34 and 52.96% respectively which were obtained under the following conditions: 100 mL of solution volume, 200 mg/L dye solution, 0.1g of adsorbent, 200 rpm agitation speed, and 24 hr-shaking duration. Therefore, the OPP was used as an adsorbent for further adsorption experiments which were carried out in batch mode as functions of contact times, initial pH, initial dye concentrations, and temperatures.

Firstly, to study the effects of contact times, a series of 250 mL Erlenmeyer flasks containing 100 mL of 200 mg/L RB solution was dispersed with 0.1 g of OPP. These flasks were plugged with parafilm to prevent evaporation and then horizontally shaken at 25±0.5°C. Samples were measured at intervals between 5 and 480 min. Secondly, to investigate the effects of initial pH, the procedure of the first experiment was repeated but the initial pH were adjusted between 2.0 and 10.0 by the addition of 0.1N NaOH and/or 0.1N HCl, and then shaken for 24 hrs. Thirdly, the effects of initial dye concentrations were determined by variations between 50 and 250 mg/L prepared and treated in the same procedure as the second experiment. Finally, to study the effects of temperature, the first and the third experiments were repeated again at the temperatures between 35 and 55 °C. All samples were filtrated through a 0.45 micron filter to remove adsorbent particles. The residual RB concentrations in the filtrate were measured using UV-Vis Spectrophotometer at the maximum wavelength (λ_{max}) at 560 nm.

2.4 Desorption experiments

The spent OPP obtained from adsorption experiments of 200 mg/L of RB solution (100 mL) with 0.1 g of adsorbent, was harvested by filtration and then dried in air for 24 hours. The OPP loaded by RB was treated with 200 mL of two solvents such as distilled water and 0.1 M HCl solution by shaking at 200 rpm for 24 hrs. The suspension was filtrated and the amount of desorbed RB in the filtrate was determined.

2.5 Adsorbent characterization

The Brunauer-Emmett-Teller (BET) surface areas were measured by a surface area analyzer using nitrogen adsorption at -196°C. Before measurement, samples were degassed (Ruthven, 1984).To resolve the functional groups

and its wave numbers, the IR-spectra of the precursor and OPP were determined by Fourier transform infrared spectrometer (FT-IR) in the range of 500-4,000 cm^{-1}. In this analysis, finely grounded sorbent was encapsulated with KBr in the ratio 1:20 to prepared the translucent sample disks. Scanning electron microscopy (SEM) characterization was carried out to observe the surface texture and porosity for the two adsorbents. The organic matter contents of dye, PP, OPP and HDTMA were determined by standard test methods for moisture, ash and organic matter of peat and organic soils, ASTM D 2974 (American Society for Testing and Materials [ASTM], 1916). The point of zero charge of OPP was also investigated in the same manner as those mentioned in literature (Umpuch & Jutarat, 2013).

3. Results and Discussion

3.1 Surface characterization of adsorbent

The N_2 adsorption isotherms measured on the PP and OPP samples (not shown) are according to type I pattern of the International Union of Pure and Applied Chemistry (IUPAC) indicating the adsorption occurred on non-porous or macro-porous surfaces. The specific surface areas of PP and OPP determined by multipoint BET analysis were 1.30 m^2/g and 1.10 m^2/g, respectively. The slightly lower BET surface area of OPP was due to the fact that the small internal surface area of PP was hindered by surfactant film coated on the external surface of the PP during adsolubilization.

The FT-IR spectra of raw PP, OPP and HDTMA are shown in Figure 2. The bands of raw PP at 3,359 cm^{-1} (stretching vibrations of the surface hydroxyl group (O-H)), 2,936 cm^{-1} (C-H_n stretching), 2,360 cm^{-1} (C≡C and C≡N stretching), 1,747 cm^{-1} (COO and C=C stretching), 1,635 cm^{-1} (COO^- stretching, indicative of pectin structure), 1,436 cm^{-1}(C-O stretching vibration), 1,260 cm^{-1}(O-H, C-H gathering), and 1,055 cm^{-1}(C-O-C stretching), respectively. The peak shifting before and after adsolubilization is also represented in Figure 2. After adsolubilization, some of the fundamental peaks of PP were shifted from their positions and there was a new peak of OPP at band 2,852 cm^{-1}, C-H stretching (aliphatic, alkane). It might be due to the surfactant formed as admicelle having long chain of alkyl groups on the precursor surface.

The SEM images of PP and OPP are shown in Figure 3a and b. A ridge texture surface without pores of PP can be observed from Figure 3a. Progressive change, thin film developing gradually on the surface, and well-developed plain structure on the surface of the OPP were observed in the Figure 3b. It may be due to the admicelle coating on the external surface of PP after adsolubilization and covering the ridge structure of PP.

The organic matter contents of RB dye, PP and HDTMA were 43.78%, 68.69%, and 99.87%, respectively. After adsolubilization, the organic matter of PP increased from 68.69% to 77.15%. The increase was attributed to the admicelle existing on the external surface of PP. From the above results, the main compositions of RB dye and OPP were organic and it was possible to take the hydrophobic interactions into account.

The point of zero charge (pzc) was interpreted from the plot of pH_0-pH_f versus pH_0 and the pzc of OPP was

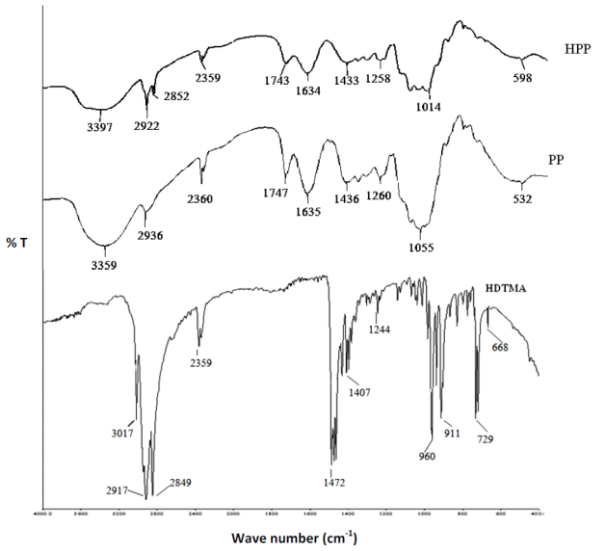

Figure 2. IR spectra of PP, OPP, and HDTMA.

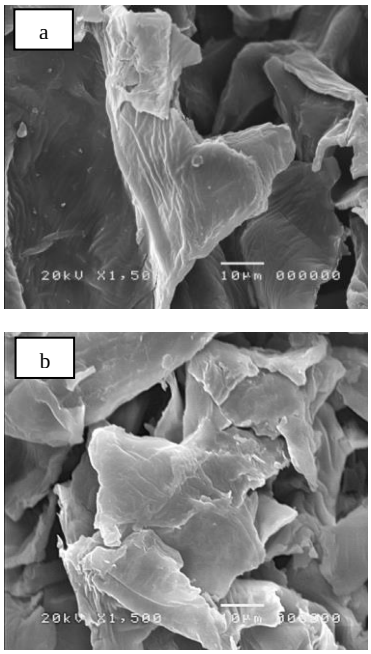

Figure 3. SEM images of PP (a) and OPP (b).

2.0. The increase of pH from 2.0 to10.0 shows more negative of pH_0-pH_f. Below the pzc, the acidic water donates more H^+ than $OH^-$and so the OPP surface is positively charged (attracting anions).

3.2 Effect of contact time

The plot of dye removal percentage versus contact time in the range of 5-480 min is presented in Figure 4. The adsorption rate was rapid in the first 20 min and then increased at a slower rate until reaching a constant at 40 min, the equilibrium stage. The high adsorption rate at the initial stage

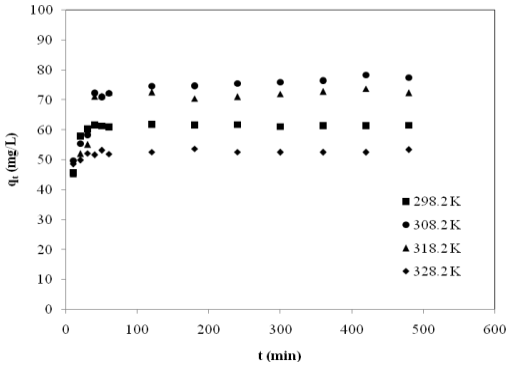

Figure 4. Adsorption kinetics of RB onto OPP at 298 – 328 K (initial concentration of RB: 200 mg/L; agitation speed: 200 rpm; dose of OPP = 0.1 g/100 mL).

was due to large availability of active sites on the OPP surface. In the latter stage, the admicelle on the adsorbent surface became almost saturated by RB dye and then the RB molecules diffused into the interior. The OPP was saturated with RB at the final stage. The high adsorption rate is beneficial in water treatment system design. In addition, the adsorption capacity at 298.2K was higher than those of 308.2 and 318.2 K. It could be explained that the thermal stabilities of RB dye and the admicelle on the biosorbent were much lost at temperature above 298.2K which may cause the degree of hydrophobicity of RB dye and the admicelle on the biosorbent was changed. Therefore, the adsorption behavior was different at the temperature above and below 298.2K.

3.3 Effect of initial solution pH and adsorption mechanisms

A most important parameter which influences adsorption is the pH of the solution. The initial pH of the solution was varied in the range of 2.0-10.0 and all other parameters were fixed. There was a sharp increase in sorption capacity with increase in pH of the RB solution from pH 2.0 to 4.0, reached a maximum at pH 6.0, and then finally decreased from pH 6.0 to 10.0 (Figure 5). The maximum sorption capacity of RB was 74.53 mg/g at pH 6.0.

The possible mechanism of RB can be explained by considering the influence of pH. At pH below 3.7 (pKa of RB), the co-ions of cationic molecules (RB) were repulsed by the fixed positively charges on the external surface of admicelle. From the pzc results, the surface of OPP above pH 2.0 was positively charged. This results in low adsorption capacity of RB (Figure 6a). As the pH increased from 2.0 to 6.0, the sorption capacity of RB increased. In solution, RB molecules (monomeric form) can ionize a proton from carboxyl group, producing the zwitterionic format pH > pKa (Guo *et al.*, 2005). The zwitterions form of RB in water may have caused the aggregation of RB molecules to form a bigger molecule (dimer) due to the electrostatic interaction between carboxylate and xanthane groups of the monomer. The dimer was neutral which was easier to enter into the admicelle body because of weakening in the electrostatic repulsion (Figure 6b). The maximum sorption capacity was observed at pH 6.0 and similar behavior was observed by the literature (Elsayed, 2009; Guo *et al.*, 2005). However, the uptake of RB slightly decreased when the pH increased from 6.0 to 10.0. This was due to the fact that high amount of OH^- in alkali medium could affect the formation of dimer and amount of the dimer was lower (Figure 6c).

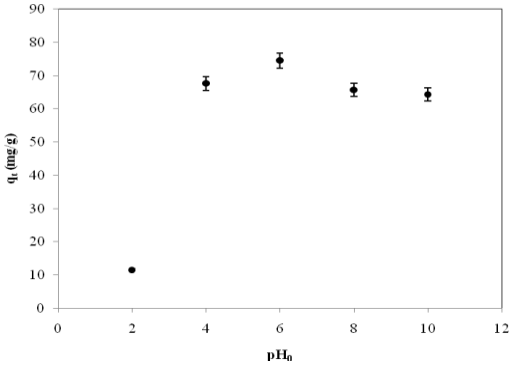

Figure 5. Effect of initial solution pH on the adsorption of RB onto OPP (initial concentration of RB: 200 mg/L; agitation speed: 200 rpm; dose of OPP = 0.1 g/100 mL).

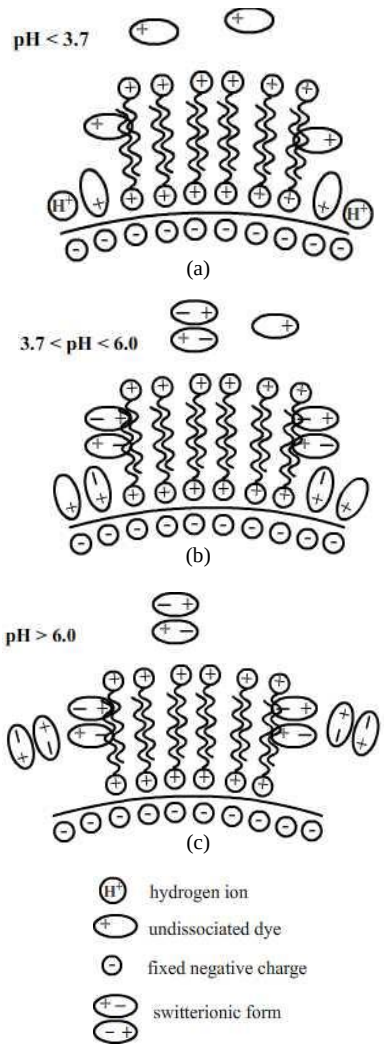

Figure 6. Adsorption mechanism of RB onto OPP.

3.4 Isotherm studies

To optimize the design of an adsorption process, analysis of the adsorption equilibrium data is important. Three isotherm equations, Langmuir, Freundlich, and Temkin isotherm models were tested for the sorption behavior of RB onto OPP. The Langmuir isotherm was used to estimate the maximum adsorption capacity corresponding to complete monolayer coverage on the homogeneous adsorbent surface without any interaction between adsorbate molecules. The linearized form of Langmuir isotherm is commonly written as

$$\frac{C_e}{q_e} = \frac{1}{k_L q_m} + \frac{C_e}{q_m} \quad (1)$$

Where q_e is the amount of RB adsorbed on the adsorbent in mg/g, C_e is the retained RB concentration at equilibrium (mg/L), q_m is a monolayer adsorption capacity expressed in mg/g, and b is the Langmuir constant which is a measure of energy of adsorption expressed in L/mg. The plots of C_e/q_e versus C_e at the different temperatures are shown in Figure 7. It was observed that the equilibrium data fitted well by the fitting lines in all cases. The values of regression coefficients and q_m obtained at different temperatures are presented in Table 1.

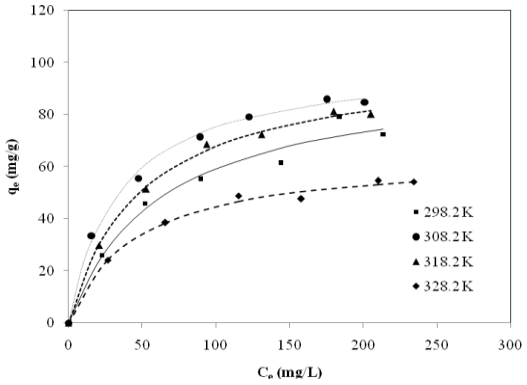

Figure 7. Adsorption isotherm of RB onto OPP at 298 – 328 K (initial concentration of RB: 50-300 mg/L; agitation speed: 200 rpm; dose of OPP = 0.1 g/100 mL).

Table 1. Isotherm constants for the adsorption of RB on OPP.

Model	Parameter	T(K)			
		298.2	308.2	318.2	328.2
Langmuir isotherm	q_{max}(mg/ g)	96.00	104.17	101.01	64.51
	k_L(L/ g)	1.54	2.92	2.06	1.45
	r^2	0.9554	0.9975	0.9968	0.9929
Freundlich isotherm	k_F(mg$^{1-1/n}$. L$^{1/n}$/ g)	2.29	3.01	2.53	2.42
	n	2.18	2.68	2.53	2.71
	r^2	0.9540	0.9783	0.9615	0.9483
Temkin isotherm	A (L/min)	0.182	0.146	0.314	0.228
	B (L/g)	21.90	21.15	22.94	13.94
	r^2	0.9920	0.9880	0.9507	0.9693

The Freundlich isotherm, which is based on heterogeneous surface and infinite surface coverage, was selected to analyze the equilibrium data. The linearized form of Freundlich isotherm is commonly written by:

$$\ln(q_e) = \ln(k_F) + \frac{1}{n}\ln(C_e) \quad (2)$$

Where q_e is the amount of RB dye adsorbed (mg/g), C_e is retained concentrations of adsorbate at equilibrium (mg/L), k_F is the adsorption capacity and 1/n is the adsorption intensity. The plots of log q_e versus log C_e at different temperatures (Figure 8). The data were well fitted by straight lines. The values of $1/n$ and k_F obtained at different temperatures are also included in Table 1.

Temkin isotherm model assumes that the heat of adsorption of all the molecules in the layer would decrease linearly with coverage due to adsorbate/adsorbent interactions. The linearized form of Temkin isotherm is commonly written by:

$$q_e = B\ln(A) + B\ln(C_e) \quad (3)$$

Where $RT/b = B$, R is the gas constant (8.314 J/mol.K) and T (K) is the absolute temperature. The constant B is related to the heat of adsorption; A is the equilibrium binding constant (L/min) corresponding to the binding energy. A plot of q_e versus lnC_e yields a linear line. The constants A and B are also given in Table 1. The good linear fitting by higher correlation coefficients indicated that there is good interaction between the adsorbate and the adsorbent.

The calculated four isotherm constants and their corresponding linear regression correlation coefficient values (r^2) at 298.2-328.2 K are given in Table 1. It can be concluded that linear fits using the three equations were good for studying the adsorption of RB dye onto OPP within the used concentration range but the fit with the Langmuir equation was comparably better. Also, it was observed that the monolayer adsorption capacity (q_m) of OPP for RB dye was found to be 64.5-104.2 mg/g. The best fit of equilibrium data in the Langmuir isotherm expression confirmed the monolayer coverage of RB dye onto OPP.

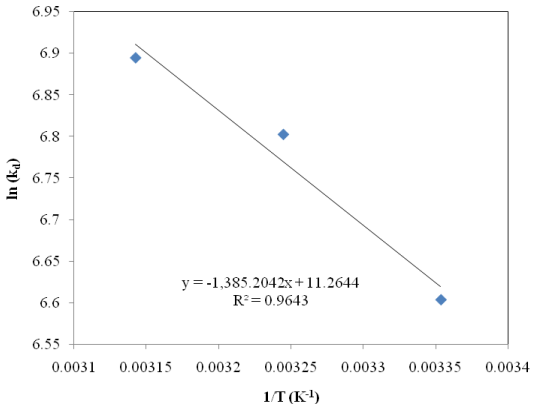

Figure 8. Plot of ln (k_d) versus 1/T

3.5 Sorption kinetics

To study the adsorption kinetics of RB dye onto OPP, three models such as pseudo-first order, pseudo-second order, and intraparticle model were used.

The linearized-integral form of pseudo-first-order kinetic model is expressed as:

$$\ln(q_e - q_t) = \ln(q_e) - k_1 t \quad (4)$$

The linearized-integral form of the pseudo-second-order model is expressed as:

$$\frac{t}{q_e} = \frac{1}{k_2 q_e^2} + \frac{t}{q_e} \quad (5)$$

Where q_e is the amount of RB adsorbed at equilibrium (mg/g), q_t is the amount of RB adsorbed at any time (mg/g), t is the agitation time (min), and k_1 and k_2 are rate constants (Table 2) of pseudo-first-order and pseudo-second order sorption respectively. The plots of log (q_e-q_t) versus t (figure not shown) and (t/q_t) versus t were used to determine the rate constants of k_1 and k_2, respectively. The linearized-integral form of intraparticle model is written as:

$$q_t = k_p t^{1/2} + C \quad (6)$$

Where k_p is the desorption constant (g/mmol) during any one experiment and$C$ is the initial RB sorption rate, in mmol/(g.min). Thus the constants can be obtained from the slope and intercept of the linear plot of q_t versus $t^{1/2}$. Equation 9 will be used to test the applicability of the intraparticle equation to the kinetics of RB sorption on the OPP.

The validity of the three kinetic models can be checked by their linearized plots. The correlation coefficient (r^2) was used to compare the applicability of different kinetic models in fitting the experimental data. Table 2 shows the corresponding parameters of the three kinetic models under different conditions. Based on r^2, the pseudo second-order kinetic model was well fitted to the experimental data.

Table 2. Kinetic model constants for RB adsorption on OPP.

Model	Parameter	T(K)			
		298.2	308.2	318.2	328.2
	q_e (exp) (mg/g)	60.40	74.68	71.20	52.17
Pseudo-first Order	k_1 x10^2 (1/min)	0.46	0.70	0.57	0.46
	q_e (cal) (mg/g)	1.00	5.29	18.09	9.96
	r^2	0.0611	0.7764	0.4372	0.0554
Pseudo-second Order	k_2 ×10^3 (g/(mg.min))	23.86	2.25	3.19	29.28
	q_e (cal) (mg/g)	61.73	78.13	73.53	52.91
	r^2	1.000	0.9992	0.9995	0.9999
Intra-particle diffusion	k_i (L/mg)	1.28	2.10	1.93	1.00
	I (L/g)	41.68	42.31	41.31	37.52
	r^2	0.2959	0.5022	0.4516	0.2504

Furthermore, the q_e calculated from the pseudo second-order kinetic model was close to the experimental data. Thus, the overall rate of RB dye adsorption process was largely controlled by the chemisorptions process.

3.6 Sorption thermodynamics

Thermodynamic parameters, such as change in free energy ($\Delta G°$), enthalpy ($\Delta H°$), and entropy ($\Delta S°$) associated to the sorption process, were obtained using the following equation:

$$\ln k_F = \frac{\Delta S^0}{R} - \frac{\Delta H^0}{RT} \quad (7)$$

Where R is the universal gas constant (8.314 J/K.mol), T is the absolute solution temperature (°C) and k_F is the distribution coefficient. The values of $\Delta H°$ and $\Delta S°$ were calculated from the slope and intercept of van'tHoff plot between lnk_F versus $1/T$ and are listed in Table 3. $\Delta G°$ and k_F were calculated using the relation below:

$$\Delta G^0 = -RT \ln k_F \quad (8)$$

$$k_F = \frac{C_{Ae}}{C_e} \quad (9)$$

Where C_{Ae} is amount of the RB adsorbed at equilibrium (mg/L) and C_e is retained concentration of each species at equilibrium (mg/L).

As seen in Table 3, all $\Delta G°$ values are negative (-16.22 to -17.09 kJ/mol) showing that RB adsorbed onto the OPP was spontaneous and the system did not gain energy from an external source. As the temperature increased, the $\Delta G°$ values shifted to a higher negative value suggesting that the adsorption was more spontaneous. In adsorption processes, a $\Delta G°$ value in the range -20 to 0 kJ/mol corresponded to physical processes, while those in the range of -80 to -40 kJ/mol corresponds to chemisorptions (Seki & Yurdakoç, 2006). Therefore, the adsorption mechanism is dominated by physisorption. From van't Hoff plot (not shown), the linear tendency was observed at temperature range of 308.2-328.2 K. The slope, ordinate intercept and correlative coefficient (r^2) were 3,328,-10.08, and 0.9963 respectively. Then, the thermodynamic parameters were calculated as shown in Table 3. The negative value of $\Delta H°$ showed the adsorption involved an exothermic process. The positive value of entropy change ($\Delta S°$) corresponded to an increase in the degree of freedom of the adsorbed species. A small change in the entropy shows that OPP does not change significantly.

Table 3. Thermodynamic constants for RB adsorption on OPP.

T(K)	k_F(L/mol)	$\Delta G°$(kJ/mol)	$\Delta H°$(kJ/mol)	$\Delta S°$(kJ/mol.K)
298.2	737.68	-16.37	-27.67	+0.0838
308.2	899.94	-16.86		
318.2	986.76	- 17.09		
328.2	694.56	-16.22		

3.7 Desorption

Desorption studies help to elucidate that nature of adsorption and recycling of the spent adsorbent and the dye. If the adsorbed dyes can be desorbed using neutral pH water, the attachment of the dye of the adsorbent is by weak bonds. If acidic or alkaline water desorb the dye, the adsorption is by ion exchange. Distilled water only desorbed 41.40 % of RB from the loaded OPP while the HCl desorbed 83.33%. Desorption of RB dye by mineral acid indicates that the dye was adsorbed onto the OPP by physisorption mechanisms. However, there was still adsorbed RB attached in the OPP with strong interactions which may be hydrophobic interactions. This showed that the adsorption was of physical nature.

4. Conclusions

This research presented some important phenomena associated with RB adsorption using OPP. The adsorption was found to be strongly dependent on pH, initial adsorbate concentration, and solution temperature. The optimum condition was observed at pH 6.0, 35°C, and 40 min. The equilibrium data were better fitted by Langmuir isotherms than Freundlich, and Temkin isotherms. Pseudo-second-order kinetic model was found to be the predominant mechanisms for RB adsorption of OPP. The thermodynamic parameters associated with the adsorption process were also evaluated. The negative value of $\Delta G°$ confirmed the spontaneous nature of RB sorption onto the OPP. The negative $\Delta H°$ values confirmed that the adsorption process was exothermic. The results indicated that OPP could be employed as an effective adsorbent for the removal of RB from the aqueous solution.

Acknowledgements

This study was financially supported by the Graduate Program in Environmental Engineering, Ubon Ratchathani University (UBU). Authors express their gratitude to the staff of the Office of International Relations at UBU for assistance with English.

References

Anandkumar, J., & Mandal, B. (2011). Adsorption of chromium (VI) and Rhodamine B by surface modified tannery waste: Kinetic, mechanistic and thermodynamic studies. *Journal of Hazardous Materials, 186*, 1086-1096.

Anastopoulos, I., & Kyzas, G. Z. (2014). Agricultural peels for dye adsorption: A review of recent literature. *Journal of Molecular Liquids, 200*, 381-389.

American Society for Testing and Materials, (1916). *ASTM D 2974-87 Standard test methods for moisture, ash, and organic matter of peat and other organic soils*. Philadelphia, PA: Author. Retrieved from: http://gsr pdf.lib.msu.edu/ticpdf.py?file=/1990s/1993/930331.pdf

Bhat, A., Megeri, G. B., Thomas, C., Bhargava, H., Jeevitha, C., Chandraskhekar, S., & Madhu, G. M. (2015). Adsorption and optmization studies of lead from aqueous solution using γ–Alumina. *Journal of Environmental Chemical Engineering, 3*, 30-39.

Guo, Y., Zhao, J., Zhang, H., Yang, S., Qi, J., Wang, Z., & Xu, H. (2005). Use of rice husk-based porous carbon for adsorption of Rhodamine B from aqueous solutions. *Dyes and Pigments, 66*, 123-128.

Hameed, B. H. (2009). Removal of cationic dye from aqueous solution using jackfruit peel as non-conventional low-cost adsorbent. *Journal of Hazardous Materials, 162*, 344-350.

Khan, S., Farooqi, A., Ihsan Danish, M., & Zeb, A. (2013). Biosorption of copper (II) from aqueous solutions using *citrus sinensis* peel and wood sawdust: Utilization in purification of drinking and waste water. *International Journal of Research in Agricultural Sciences, 16*(2), 297-306.

Ma, L., Xi, Y., He, H., Ayoko, G. A., Zhu, R., & Zhu, J. (2016). Efficiency of Fe-montmorillonite on the removal of Rhodamine B and hexavalent chromium from aqueous solution. *Applied Clay Science, 120*, 9-15.

Pagnanelli, F., Minelli, S., Veglio, F., & Toro, L. (2013). Heavy metal removal by olive pomace: Biosorbent characterisation and equilibrium modeling. *Chemical Engineering Science, 58*, 4709-4717.

Pehlivan, E., & Altun, T. (2007). Ion-exchange of Pb^{2+}, Cu^{2+}, Zn^{2+}, Cd^{2+},and Ni^{2+} ions from aqueous solutions. *Chemical Engineering Journal, 148*, 68-79.

Rao, K. S., Mohapatra, M., An, S., & Venkateswarlu, P. (2010). Review on cadmium removal from aqueous solutions. *International Journal of Environmental Science and Technology, 2*, 81-103.

Ruthven, D. M. (1984). *Principles of adsorption and adsorption processes*. New York, NY: John Wiley and Sons.

Schiewer, S., & Iqbal, M. (2010). The role of pectin in Cd binding by orange peel biosorbents: A comparison of peels, depictinated peels and pectin acid. *Journal of Hazardous Materials, 177*, 899-907.

Seki, Y., & Yurdakoç, K. (2006). Adsorption of promethazine hydrochloride with KSF montmorillonite. *Adsorption, 12*(1), 89-100.

Tasaso, P. (2014). Adsorption of copper using pomelo peel and depectinated pomelo peel. *Journal of Clean Energy Technologies, 2*, 154-157.

Umpuch, C. (2015). Removal of Yellow20 dye from aqueous solution using organo-rice straw: Characteristic, kinetic and equilibrium studies. *Engineering Journal, 19*, 59-69.

Umpuch, C., & Sakaew, S. (2013). Removal of methyl orange from aqueous solutions by adsorption using chitosan intercalated montmorillonite. *Songklanakarin Journal of Science and Technology, 35*, 451-459.

Umpuch, C., & Jutarat, B. (2013). Adsorption of organic dyes from aqueous solution by surfactant modified corn straw. *International Journal of Chemical Engineering and Applications, 4*, 41-59.